Available online at www.sciencedirect.com
ScienceDirect
Engineering Structures 30 (2008) 1922–1937
ENGINEERING STRUCTURES
www.elsevier.com/locate/engstruct

Performance of AASHTO girder bridges under blast loading

A.K.M. Anwarul Islam[a,*], Nur Yazdani[b,1]

[a] Department of Civil & Environmental Engineering, Youngstown State University, 2460 Moser Hall, One University Plaza, Youngstown, OH 44555, United States
[b] Department of Civil & Environmental Engineering, University of Texas at Arlington, Box 19308, 425 Nedderman Hall, Arlington, TX 76019, United States

Received 20 June 2006; received in revised form 14 December 2007; accepted 19 December 2007
Available online 1 February 2008

Abstract

AASHTO has specified probability-based design methodology and load factors for designing bridge piers against ship impact and vehicular collision. Currently, no specific AASHTO design guideline exists for bridges against blast loading. Structural engineering methods to protect infrastructure systems from terrorist attacks are required. This study investigated the most common types of concrete bridges on the interstate highways. A 2-span 2-lane bridge with Type III AASHTO girders was used for modeling. AASHTO Load and Resistance Factor Design methods were used for the model bridge design. The girders, pier caps and columns loading were analyzed for probable blast loading. The model bridge failed under the probable blast loads applied over and underneath the bridge. The research findings show that typical AASHTO girder bridges are unable to resist probable blast loads.
Published by Elsevier Ltd

Keywords: Blast; Explosion; Bridge design; Terrorism; AASHTO girders

1. Introduction

Recent terrorist attacks around the world have created concern over the safety and protection of the public and the nation's infrastructure. Bridges are the most common infrastructures in the nation's highway system. As a result of the terrorist threats and attacks, engineers and transportation officials are becoming more active in physically protecting bridges from potential blast attacks. Approximately 90% of the prestressed girder bridges in Florida are American Association of State Highway and Transportation Officials (AASHTO) type girder bridges. It is likely that these bridges were not designed to resist explosive impact.

The recent heightened awareness of terrorist activities and rising insurance costs have resulted in a drastic increase in the demand for structural consequence evaluations and engineering designs of buildings and structures subject to explosive load. Advances in process and structural engineering now make it possible to design and analyze buildings subject to external blast load from accidental explosions and terrorist bombs with acceptable accuracy. Conventional bridge structures normally are not designed to resist blast load. Since the magnitudes of potential explosive load are significantly higher than other design loads, conventional structures are more susceptible to damage from explosions. Important bridges on the highway system have greater chances of being potential target for terrorist explosions to disrupt traffic movement, to cause human casualties and to impact socio-economic condition.

Since the 2001 terrorist attacks, numerous research and demonstration initiatives have been undertaken to find cost-effective and efficient retrofit, security and rapid reconstruction techniques for important buildings. The bridge and highway infrastructure engineers face new challenges relating to the security of critical structures against terrorists attacks. In response to this need, the AASHTO Transportation Security Task Force sponsored the preparation of a guide to assist transportation professionals in identifying critical highway structures and to take action to reduce their blast vulnerability. In order to provide guidance to bridge owners and operators, the Federal Highway Administration (FHWA) formed the Blue Ribbon Panel [1] on bridge and tunnel security. The panel's report includes recommendations on actions that can be taken by bridge and tunnel owners and operators or by

* Corresponding author. Tel.: +1 330 941 1740; fax: +1 330 941 1740.
E-mail addresses: aaislam@ysu.edu (A.K.M. Anwarul Islam), yazdani@uta.edu (N. Yazdani).
[1] Tel.: +1 817 272 5055; fax: +1 817 272 2630.

0141-0296/$ - see front matter Published by Elsevier Ltd
doi:10.1016/j.engstruct.2007.12.014

Notation

The following symbols are used in this paper:

A	axial failure;
DL	dead load;
E_c	modulus of elasticity of concrete;
EV	extreme event load;
f_c	28-day compressive strength of concrete;
LL	live load;
M	moment failure;
R	distance of target from point of explosion;
V	shear failure;
W	equivalent TNT weight of explosive;
W_c	unit weight of concrete;
W_T	total load;
Z	scaled distance.

FHWA, and other state and federal agencies, that will result in improved security and reduced vulnerabilities for critical bridges and tunnels. Additionally, to develop and transfer knowledge rapidly within the bridge community, a series of workshops were conducted in early 2003 under the National Cooperative Highway Research Program (NCHRP) Project 20–59(2).

AASHTO has probability-based design methodology for designing bridges for various dynamic loads such as seismic, ship impact and vehicular collision. However, it has no specific guidelines for the design of bridges for blast loading. In response to this vital need and growing concern about the safety of highway bridges, NCHRP has sponsored a research project to develop design and detailing guidelines for blast resistant highway bridges that can be adopted in the AASHTO Bridge Design Specifications [2].

The American Society of Civil Engineers (ASCE) developed design guidelines entitled "Design of Blast Resistant Buildings in Petrochemical Facilities" [3]. This report provides general guidelines for structural design of blast resistant petrochemical facilities.

The National Center for Explosion Resistant Design [4] at the Department of Civil and Environmental Engineering at the University of Missouri-Columbia has been offering courses on "Explosion Effects and Structural Design for Blast". The course focuses on the fundamentals of explosion effects, determining blast loads on structures, computing structural response to blast loads, and the design and retrofit of structures to resist blast effects.

Researchers at the University of Texas at Austin have been developing performance-based blast design standards for bridge substructures. The goal of their research, as collected from Wessex Institute of Technology Press [5], UK, is to investigate economical, unobtrusive and effective methods to mitigate the risk of terrorist attacks against critical bridges.

Bridges are less protected as compared to other structures such as high-rise buildings, federal and state offices, and other important structures. As traffic flow continues over the interstate and state highways 24 h a day, it is a common perception that the bridges are protected to some extent by the moving traffic. The government has adopted the utmost security measures for protecting important bridges in the United States, such as the Golden Gate Suspension Bridge in San Francisco, Sunshine Skyway Cable-Stayed Bridge in Tampa, and the Brooklyn Suspension Bridge in New York City. On the other hand, typical interstate and highway bridges are largely unprotected and vulnerable to terrorist attack.

The passive protection of public buildings to provide life safety in the event of explosions is receiving renewed attention. This highly effective approach of blast resistant design is only feasible where a standoff zone is available and affordable. For many urban settings, the proximity to unregulated traffic brings the terrorist threat to or within the perimeter of the building. For these structures, blast protection has the more modest goal of containing damage in the immediate vicinity of the explosion and the prevention of progressive collapse. In suburban and government facilities, the minimum standoff zone can be easily established. In the urban area, it is relatively harder to attain these standoff distances surrounding the facilities.

AASHTO girder, suspension, cable-stayed and box girder bridges are the most commonly used concrete bridge types. Because of the complex nature of suspension, cable-stayed or box girder bridges, and less possibility of blast attack as they are well-protected due to their importance, the blast performance of an AASHTO girder bridge was investigated herein. The vast majority of typical unprotected highway concrete bridges in this country fall under this category. The intent of this study was to investigate the performance of a typical AASHTO girder bridge under probable blast loading. The results will help to determine necessary structural design criteria or retrofit techniques to reduce the probability of catastrophic structural failure, which in turn will lessen human casualties, economic losses and socio-political impact in case of blast occurrence.

2. Model bridge

A typical Type III AASHTO girder simply supported bridge of 24.38 m span length, common for Type III AASHTO girders, was selected for this study. The model bridge was assumed to contain two 3.66 m lanes, 3.05 m and 1.83 m shoulders, and two 457 mm wide barriers, producing an overall bridge width of 13.11 m. Seven simply supported Type III AASHTO girders with center-to-center spacing of 1.83 m were used at each span of the model bridge. Concrete diaphragms with total thickness of 762 mm were used to enhance continuity of the superstructure over the pier. No intermediate diaphragms were used in the model bridge.

Clear curb-to-curb roadway width of 12.19 m was used in the design. The bridge overhang width was 1.07 m with a clear distance of 610 mm between exterior girder centerline and gutter line. The perspective view, cross-section, elevation, and section at interior support showing the diaphragm of the model bridge are shown in Fig. 1. The girders sit on the bearing pads at the end bents and pier, and are considered simply supported at each span. In the model bridge, the superstructure

is assumed anchored with the pier cap through the bearing pads. The girders are connected with a 203 mm thick cast-in-place concrete deck slab, which is continuous over the pier. Seven 457 mm square prestressed precast concrete piles, spaced at 1.83 m, supported each end bent. Two identical columns of 1.07 m diameter on two separate footings supported the pier cap. Four 610 mm square prestressed concrete piles supported each footing of dimension 3.05 m by 3.05 m with the column located at the center of the footing.

The end bent cap width of 914 mm and pier cap width of 1.22 m were determined to be appropriate for this model. The designed depth of the pier cap was 1.22 m. Two columns of 1.07 m diameter each were structurally capable of supporting the bridge.

3. Failure criteria

Failure criteria can be used in combination with information about stresses in a structure to predict the load levels a structure can withstand before failure. The failure criteria at the time a structure fails can be assumed as a function of the applied loads and the material property of the element. A widely accepted general failure criterion was followed in this study — if the applied load parameter exceeds the capacity of the section, the component fails.

The highway departments categorize damaged bridge structures as partially or completely out of service based on the location, extent and intensity of damage. It was assumed herein that a bridge might collapse due to the individual failure of one or more of the main structural components — deck, beam, pier or column. Deck failure may not lead to a total collapse of a bridge because of its high redundancy and localized mode of failure, but it may cause the structure to be completely out of service. Column or pier cap failure may also initiate total collapse of a bridge making it out of service, while localized failure of a girder may not cause complete collapse.

Bridge columns are more vulnerable to blast attack because of their easy access and more likely to be attacked due to their importance in structural stability. Therefore, they are considered the most critical element of a bridge structure in terms of failure and stability. Columns are more accessible and susceptible to damage in case of a ground-based or water-borne blast attack underneath the bridge. Although one column failure may or may not initiate a bridge collapse due to possible catenary action of the bridge deck, it is considered unacceptable for vehicular movement. Failure of both columns will definitely collapse the entire model bridge.

The deck slab of a bridge is also highly vulnerable to blast attack because of its close proximity to moving vehicles. It is integrally built with the girders underneath, and secured at both edges with traffic railing barriers. The deck slab is more susceptible to damage in case an explosion originates under the bridge, as compared to an over-the-bridge explosion. Under-the-bridge explosion creates confining pressure in between girders under bridge deck that increases the deck damage, whereas over-the-bridge explosion usually occurs in the open air that facilitates escape of explosive pressure thus reducing

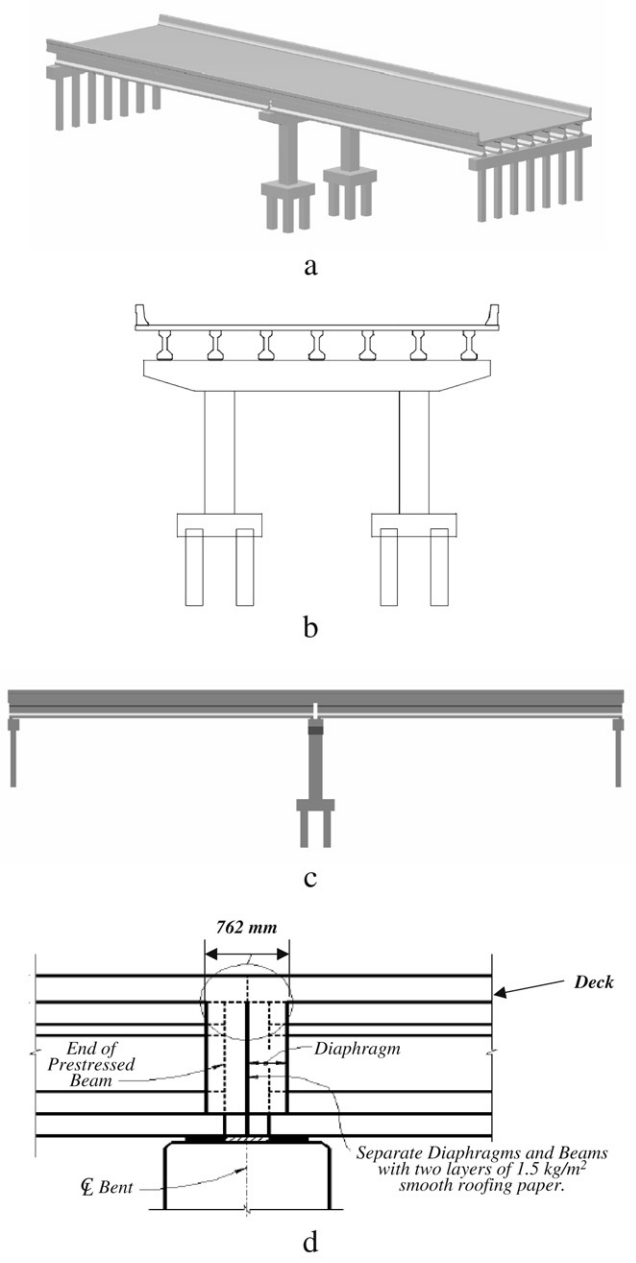

Fig. 1. Model bridge — (a) perspective view, (b) cross-section, (c) elevation, and (d) section at interior support showing diaphragm (Courtesy: FDOT, modified).

damage to bridge deck. Because of the spherical pressure profile of blast load and high redundancy of the deck slab, damage may occur on a portion of the deck slab.

The girders play an important role in securing the superstructure and substructure by creating redundancy against sudden collapse. Girders are typically designed to withstand moments and shears caused by vertically downward loads. On the other hand, a vertically upward load, caused by blast load from underneath the bridge, will cause negative moments and shears. The composite action of the deck–girder system will increase negative moment capacity of the section to a minor extent. The deck slab will contribute to most of the resistance.

The girders will have minimal resistance because they are primarily designed for positive moments.

The bridge component damage may be categorized as slight to moderate and extreme depending on the amount of damage. Minor cracking and spalling in the concrete can be easily repaired, and be considered as slight to moderate damage for which the structure may be considered partially out of service. In partially out of service bridges, traffic will be allowed to move over designated parts of the bridge, while repair work is ongoing. Because of the extreme nature of blast loading, the damage may be extreme, which may put the bridge completely out of service. In this case, traffic will be moved through an alternate route until the replacement bridge is put into service.

In case of the pier cap or column failure, there is a good chance that the whole bridge will be out of service. Individual girder failure may result in partial loss of bridge service, while more than one girder failure may force the bridge to be completely out of service. In the event of two adjacent girders with deck slab failure, the bridge may be partially out of service, which may allow one lane of traffic movement. Greater levels of damage will most likely result in complete bridge closure until a full replacement is performed.

4. Model bridge design and element capacity

All major components of the model bridge were designed following AASHTO Load and Resistance Factor Design (LRFD) Bridge Design Specifications, 2nd Edition, 1999, with Interims through 2003 [6]. The capacity of each element was determined from the design and later compared with the applied loads on the respective element to determine its performance. The respective capacity of each individual element was determined using simple support condition for the girders, and fixed support condition for connection between the pier cap and the columns.

4.1. Deck slab

Following the Empirical Method of the AASHTO LRFD Bridge Design Specifications, the deck slab was designed with #5 reinforcement spaced at 305 mm on center at top and bottom in both directions. The deck slab had a clear cover of 50 mm at top and bottom. In addition to this typical reinforcement, additional reinforcement on top of the deck perpendicular to the direction of traffic was also used to secure connection between the barrier and the deck. To resist the negative flexure over the pier support, additional steel along the direction of traffic was used at the top of the slab extended up to 6 m in both directions from the pier cap. The diaphragms at beam ends were also nominally reinforced.

4.2. AASHTO girder

Type III AASHTO girders were designed using the Florida Department of Transportation (FDOT) LRFD Prestressed Beam Design Program [7]. The girders were prestressed with 13 mm diameter 1862 MPa low relaxation 30 straight strands of which 4 strands were debonded for 3.96 m at each end. The jacking force per strand was limited to 138 kN. The ratio of the ultimate moment capacity to the moment resulting from the applied pressure due to LRFD Strength I loading was 1.17. Therefore, the girder design was acceptable under normal traffic loading.

Prestressed girders composite with the deck slab react with their fullest capacity against vertically downward loads resulted from over-the-bridge explosion. As girders are connected with the deck slab through horizontal shear reinforcement, girder–slab composite section exhibits single T-beam properties with the girders prestressed to enhance positive moment capacity. From the beam design output, the maximum positive moment capacity of the prestressed girder was 6.10 MN m, while the maximum shear force capacity was 1.24 MN.

When the bridge deck experiences vertically upward loads generated through an explosion underneath the bridge, the girder–slab composite is subjected to negative moments. In this situation, the prestressing steel located near the bottom flange is ineffective in providing the needed tensile strength. Only the non-prestressed longitudinal reinforcement in the slab provides limited tensile strength. Manually analyzing the section properties of an inverted T-beam, the maximum negative moment capacity of the girder–slab composite was determined as 1.09 MN m. The shear capacity of the girders remained unchanged at 1.24 MN.

4.3. Pier cap

The pier cap and the end bent cap were designed using commercially available software RC-Pier [8]. Multiple piles support the end bent caps with short spans between the piles, which decreases the resulting moment and increases the cap stiffness. Moreover, the bottom of the end bent caps stays in touch with the ground. This makes them less critical and more protected compared to the pier cap in assessing the bridge performance. Therefore, end bent caps were excluded from this study. The pier cap was reinforced with 13 #10 bars at top and bottom with 75 mm typical clear cover at each side. Two-leg #5 double stirrups spaced at 150 mm on the center were also used to satisfy vertical shear and torsion. The ratio of the resisting moment to the resulting moment caused by regular dead and live load was 1.9, which exceeds the acceptable limit of 1.

When an explosion occurs right near the column base, vertically upward loads produce very high negative moment on the cap. For an explosion over the pier cap, a very high positive moment is applied on the cap. As the pier cap was reinforced with identical reinforcement at top and bottom, the flexural capacity of the pier cap against positive or negative moment is the same. From RC-Pier output, the maximum resisting positive or negative moment of the pier cap was 4.00 MN m. The maximum shear strength was 3.43 MN.

4.4. Column

The columns and the footings were also designed using the RC-Pier. Minimum reinforcement requirement governed in the column steel selection. Since columns are possibly the most

critical component of the bridge, they were reinforced with the maximum permissible reinforcement of 20 #10 bars with single #4 ties spaced at 305 mm, so that the maximum efficiency of the columns could be achieved. The ratio of the ultimate moment capacity to the resulting moment due to normal traffic loading was 1.29, which is within the acceptable range.

Using the FDOT Biaxial Column Program [9], the maximum resisting moment and axial capacity of the column under combined compression plus bending were determined as 3.28 MN m with 8.90 MN axial load. Footings and piles were not considered as critical components of failure as they were buried underground.

5. Blast load

The initial step in blast design or analysis is the determination of the blast load. Blasts can create very powerful and extreme loads. Even a small amount of explosive can inflict sizeable amount of damage to a structure if they are set at critical locations. Blast pressure can create loads on structures that are many times greater than normal design loads. Dynamic pressure may continue to cause drag loads on the structural frame that is left standing. If explosion occurs on top of the bridge, deck slab experiences the downward thrust of the overpressure, which is transmitted to the supporting girders, pier caps and columns. If blast load is applied at the bottom of the bridge, pier caps, prestressed girders and deck slab will be subjected to vertically upward pressure, for which they are not generally designed.

5.1. Equivalent static load

The method of determining equivalent load due to a blast explosion is a complex phenomenon. The blast pressure diminishes with distance from the point of explosion. In the TM 5-1300 Manual, Structures to Resist the Effects of Accidental Explosions, developed by the US Department of Defense [10], an empirical formula, as shown in Eq. (1), was used to find the scaled distance. The amount of blast pressure generated due to an explosion is inversely proportional to the scaled distance, which is presented in a chart form in the TM 5-1300 Manual. The empirical formula for the scaled distance, Z, is:

$$Z = \frac{R}{W^{\frac{1}{3}}}, \tag{1}$$

where, R = Distance of target from point of explosion, and W = Equivalent TNT weight of explosive.

Using this formula and the chart in TM 5-1300, Applied Research Associates, Inc (ARA) developed a software named ATBlast [11] to calculate the blast loads for known values of charge weight and standoff distance. The ATBlast software is widely used and recommended by professionals to determine the equivalent blast pressure due to an explosion. In fact, ATBlast was developed for the US General services Administration. ATBlast estimates the developed blast loads during an open-air explosion. The software allows the user to input the minimum and maximum range, increment, explosive charge weight, and the angle of incidence. From this information, ATBlast calculates the following values: Range Distance (m), Shock Front Velocity (m/ms), Time of Arrival (ms), Pressure (MPa), Impulse (MPa ms), and Duration (ms). The results are displayed in a tabular format and can be printed. In addition, the resulting pressure and impulse curves can be displayed graphically. ATBlast is a proprietary software developed by ARA, and is provided at no cost to the users.

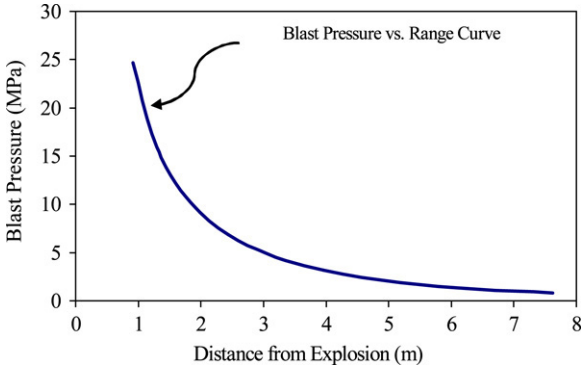

Fig. 2. Variation of pressure with distance from explosion.

In this study, ATBlast was used to convert blast loads into equivalent static loads. From Table 3 of the Blue Ribbon Panel Report on Bridge and Tunnel Security [1], the highest possibility of a conventional truck bomb is with an amount of 226.8 kg of trinitrotoluene (TNT) explosive. Therefore, the model bridge herein was assumed to be affected by this amount of TNT.

For an explosion underneath the bridge, it is reasonable to assume that a regular truck or any other vehicle commonly used to carry explosive charges cannot go closer than 1.22 m to a bridge column, and this minimum standoff distance from the point of explosion to the column surface was used herein. The maximum range used in this model analysis is 7.62 m, beyond which the impact of the probable explosion is found negligible. The typical minimum vertical clearance of 4.88 m between the bottom of the Type III AASHTO girder and the top of the roadway underneath was considered in the analysis. The bottom of the girder and the deck slab were determined to be 3.96 m and 5.18 m away, respectively, from the point of explosion, considering the charge was placed on the truck bed at 914 mm above the ground. On the other hand, when explosion occurs on top of the bridge deck, the truck bed, where the explosive is placed, also acts as a barrier between the explosion and the deck surface. Considering this barrier effect and 914 mm height of the truck bed from the deck surface, it was conservatively assumed that the minimum distance between the point of explosion and the deck surface was 1.83 m.

To obtain the loads for the model bridge, 226.8 kg of TNT with minimum and maximum ranges of 1.22 m and 7.62 m, respectively, was converted into equivalent static loads using ATBlast at every 305 mm increment. The resulting static loads, presented in Table 1, were applied on the model bridge at different critical locations. Fig. 2 illustrates variation of pressure with respect to distance from the point of explosion.

Table 1
Equivalent static pressure for 226.8 kg of TNT explosion

Range (m) (1)	Pressure (MPa) (2)
0.91	24.66
1.22	17.31
1.52	12.99
1.83	10.20
2.13	8.26
2.44	6.83
2.74	5.74
3.05	4.88
3.35	4.18
3.66	3.61
3.96	3.14
4.27	2.75
4.57	2.42
4.88	2.14
5.18	1.90
5.49	1.69
5.79	1.51
6.10	1.36
6.40	1.22
6.71	1.11
7.01	1.00
7.32	0.91
7.62	0.83

Closer proximity of explosion to the structure produces more severe resulting pressure and the likelihood of increased structural damage.

Fig. 3 shows the plan and elevation views of a typical blast pressure distribution on the bridge surface. If the explosion occurs 1.83 m above the deck surface, the spherical distribution of pressure extends 3.05 m in each direction as shown in the figure assuming a 30 degree angle of projection of the pressure wave.

Since blast pressure is spherical in nature, impact of pressure on the surface decreases with pressure becoming parallel to the surface under attack, while pressure applied perpendicular to the surface has the highest impact. It was assumed that a streak of pressure that makes approximately 30 degree or less angle with the surface under attack would strike the surface with less impact and diminish through reflecting on the surface. In order to simplify the method of blast distribution, it was assumed that the blast pressure beyond the 30 degree projected region has negligible impact on the structure. Weighted average of the vertical components of these inclined pressures on each girder was calculated according to the distribution shown in Fig. 3. The greatest pressure is 10.2 MPa, generated due to an explosion of 226.8 kg of TNT at a height of 1.83 m above the deck. Girder B, directly under the point of explosion, experiences the highest average pressure of 5.1 MPa for a length of 6.10 m, which is approximately 50% of the peak pressure of 10.2 MPa. The adjacent girders A and C are subjected to 3.06 MPa pressure along a length of 6.10 m, which is approximately 30% of the peak pressure. These assumptions were verified for three different intensity of explosions (226.8 kg, 45.4 kg and 22.7 kg of TNT) and were found to be acceptable. Therefore, they were used in applying average blast pressure for different load cases on the bridge components. The mathematical verifications of these assumptions were performed using MathCAD and ATBlast software, and are attached in Appendix A.

Table 2
Concrete material properties used in model bridge design and analysis

Concrete designation (1)	Element (2)	f_c (MPa) (3)	Poisson's ratio (4)	W_c (kg/m^3) (5)	E_c (MPa) (6)
Material 1	Girders Bent cap	44.82	0.2	2400	33,700
Material 2	Pier cap Columns	37.92	0.2	2400	31,000
Material 3	Deck slab	31.03	0.2	2400	28,040

f_c = 28-day compressive strength of concrete.
W_c = Unit weight of concrete.
E_c = Modulus of elasticity of concrete.

6. FEA bridge model

The model bridge was created using the STAAD.Pro [12] software for analysis, as shown in Fig. 4. The girders were coded in as beam elements and the deck slab was modeled as plate elements. The beam and the plate elements were connected at nodal points to assure strain compatibility and composite actions. A total of 58 beam elements and 128 plate elements were used in the model.

Beam elements 1 to 8 and 17 to 24 formed two end bent caps, and 9 to 16 made up the pier cap. The barriers consisted of beam elements 25, 33, 34 and 42. The girders were represented by beam elements 26 to 32 (girders 1 to 7) in the first span and 35 to 41 (girders 8 to 14) in the second span. The piles supporting the end bent caps consisted of beam elements 43 to 49 and 52 to 58. Beam elements 50 and 51 represent column 1 and column 2, respectively.

Cross-sections of all the beam elements were defined as per the geometry of the respective members. The equivalent areas of the girders and barriers were coded in the software because of their irregular shapes to account for the dead loads. The girders were modeled as pin supported on the end bent caps. The piles and the columns were modeled as fixed supported at a depth of 4.88 m from the centerline of the cap. The deck slab was made integral with the girders to represent the composite behavior.

The girders, end bents and pier cap including the columns, and the deck slab were assumed to be made of concrete Material 1, Material 2 and Material 3, respectively, with properties defined in Table 2. Although the concrete modulus of elasticity does not affect the resulting moment and shears, it affects the magnitude of stiffness and displacements. Displacement and camber of girders are normally considered for traffic riding comfort, rather than predicting member efficiency. Therefore, in assessing the performance of the model bridge, displacement was not considered as a part of the analysis.

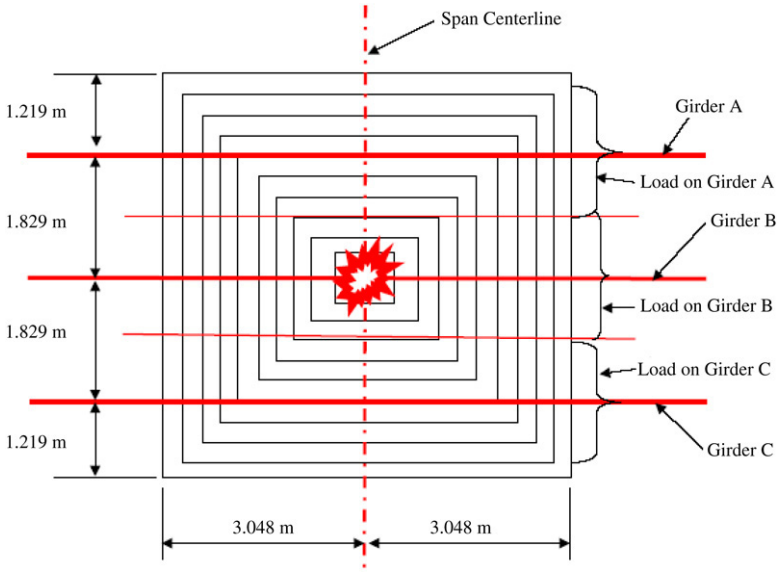

(a) Plan of bridge deck.

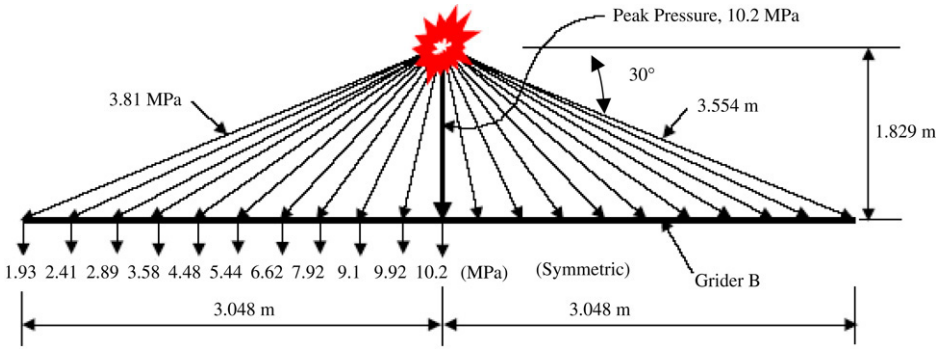

(b) Elevation of bridge deck.

Fig. 3. Plan and elevation of blast pressure distribution on bridge deck.

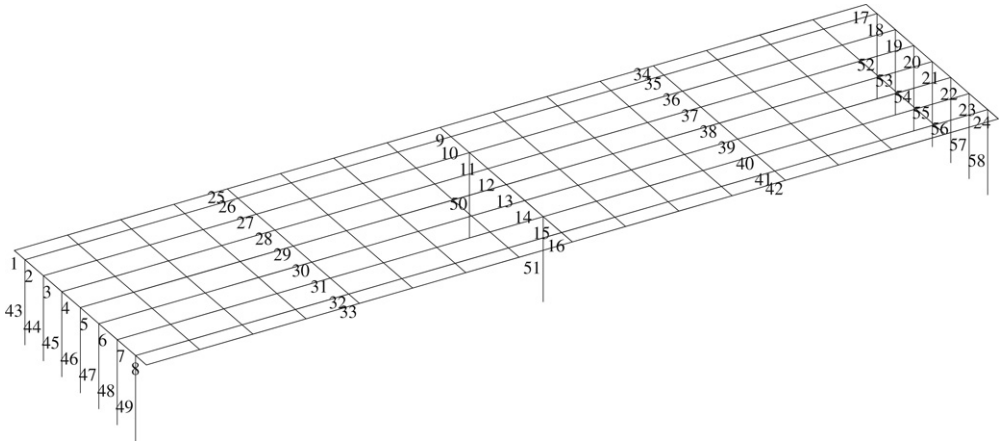

Fig. 4. Model bridge in STAAD.Pro.

6.1. *Locations of blast load application*

The deck slab is mostly affected due to possible explosion on top of the bridge. It is a highly redundant member due to the presence of alternate load paths and integral connection with the girders through horizontal shear reinforcement. Any possible slab damage due to blast is likely to be localized. The loads are distributed on the deck slab and ultimately applied as uniformly

Table 3
Critical load cases for model bridge analysis

Load cases (1)	Location (2)	Members affected (3)	Blast set-backs (4)
1	Under the bridge, at mid-span	Deck slab, girders	914 mm above ground
2	Over the bridge, at mid-span	Deck slab, girders	1.83 m above deck
3	Over the bridge, over pier cap	Deck slab, girders, pier cap	1.83 m above deck
4	Over the bridge, at span end	Deck slab, girders	1.83 m above deck
5	Under the bridge, at 1.22 m away from column	Column, pier cap	914 mm above ground

Table 4
Member status under various load cases

Location (1)	Member (2)	Load cases (3)				
		1	2	3	4	5
	Girder 1	*M*	*M*		*M*	
	Girder 2	*M*	*M*, *V*		*M*	*M*
	Girder 3	*M*, *V*	*M*, *V*	*V*	*M*, *V*	*M*
Span 1	Girder 4	*M*, *V*	*M*, *V*	*V*	*M*, *V*	*M*
	Girder 5	*M*, *V*	*M*, *V*	*V*	*M*, *V*	*M*
	Girder 6	*M*	*M*, *V*		*M*	*M*
	Girder 7	*M*	*M*		*M*	
	Girder 8		*M*		*M*	
	Girder 9		*M*		*M*	*M*
	Girder 10		*M*	*V*	*M*	*M*
Span 2	Girder 11		*M*	*V*	*M*	*M*
	Girder 12		*M*	*V*	*M*	*M*
	Girder 13		*M*		*M*	*M*
	Girder 14		*M*		*M*	*M*
	Pier cap	*M*, *V*	*M*, *V*	*M*, *V*	*M*, *V*	*M*, *V*
	Column 1	*M*	*M*, *A*	*M*, *A*	*M*, *A*	
	Column 2	*M*	*M*, *A*	*M*, *A*	*M*, *A*	*M*, *A*

M — moment failure.
V — shear failure.
A — axial failure.
Blank — survived explosion.

distributed loads along the centerline of the girders. Thus, the deck slab performance was excluded from this study in order to focus on the more critical elements of failure, such as girders, pier cap and columns.

Blast load on structures has no definite direction of application. It can affect the structure from any direction at any angle. For the sake of simplicity, only the governing vertical or horizontal components of the inclined loads were applied at critical locations on the members, as explained in the next section.

7. Blast load cases and bridge performance

The 226.8 kg explosive load was considered as an extreme event load for which the load factor is 1.00 according to the AASHTO LRFD Bridge Design Specifications [6]. In addition to these blast loads, self-weight of the structure was also considered and multiplied by a factor of 1.25. The AASHTO LRFD combination of dead and live loads for extreme event cases is presented in Eq. (2). The truck live load was not considered in the analysis for simplicity; it is negligible compared to the effect of blast load.

$$W_T = 1.25(DL) + 0.50(LL) + 1.00(EV), \quad (2)$$

where, W_T = Total load, DL = Dead load, LL = Truck live load, and EV = Extreme event load.

Converted blast pressures from Table 1 were categorized into 5 different load cases depending on the location of blast, intensity and the amount applied on a specific location, as presented in Table 3. The blast pressures were converted into uniformly distributed loads and applied along the centerline of the members for ease of load application. The tributary distribution of blast pressures was applied herein.

The model bridge was analyzed for the 5 load cases chosen herein. From the STAAD.Pro output, the maximum resulting moment and shear forces on the critical elements of the bridge were determined, and compared with their respective capacities to assess their performance. The maximum resulting moment, shears and the capacity of each critical member under consideration were tabulated in the member status Table 4 with their respective survival or failure conditions. Depending on the damage and failure conditions, the whole structure was identified as partially or completely out of service following failure criteria as defined earlier.

7.1. Load case 1

This load case assumed explosion underneath the bridge at girder mid-span, as shown in Fig. 5. The middle girder (girder 4), which is 3.96 m above the explosion, experienced a vertically upward blast pressure of approximately 1.59 MPa (Table 1, using 50% distribution) for a length of 6.10 m. This load was converted into a uniformly distributed load of 885 kN/m using girder bottom width of 559 mm. The other two girders 3 and 5 experienced 896 kPa pressure (Table 1, using 30% distribution), which is equivalent to 500 kN/m, for a length of 6.10 m. Approximately 1.22 m wide and 6.10 m long portion of the slab between the two adjacent girders, located at an inclined distance of 5.18 m, experienced a pressure of 551 kPa (Table 1, using 30% distribution), which is equivalent to 671 kN/m. In the STAAD.Pro model, these loads were applied in the middle 6.10 m of the span. The direct impact of this explosion on the pier cap and columns was neglected because of high distances from these members from the point of explosion and presence of the deck slab as a barrier.

Due to this load case, it was evident from the analysis that girder 4 experienced the maximum effect, and the adjacent two girders, 3 and 5, were subjected to less impact. From the STAAD.Pro output, the maximum negative moment and shear force on girder 4 are 27.7 MN m and 5.7 MN, respectively. Maximum negative moment and shear force on girders 3 and

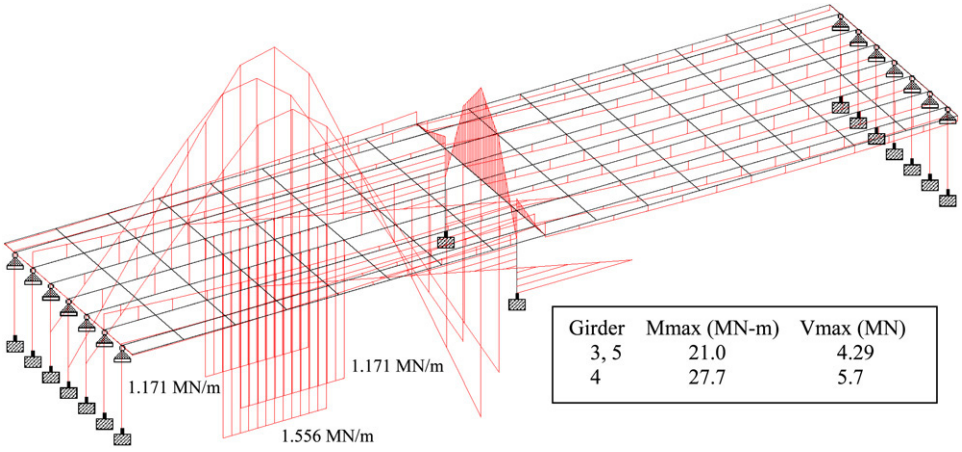

(a) Load and moment diagram.

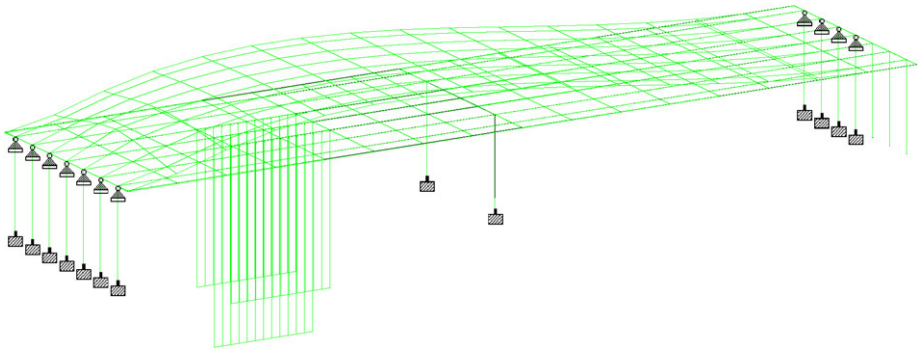

(b) Deflection diagram.

Fig. 5. Load, moment and deflection diagrams for Case I blast load.

5 were 21 MN m and 4.29 MN, respectively. The moment diagrams produced by these loads are presented in Fig. 5(a). Fig. 5(b) shows the deflection diagram for the slab/girder.

A larger positive moment of 34.27 MN m was produced at the end of girder 4 due to Case 1 load. It was due to the continuity of the girders assumed in the model over the pier cap. Although the actual support condition of the girders at the pier cap location is not fully continuous, a good amount of continuity exists as a result of the girder–slab composite action, continuity of the slab over the pier cap and diaphragms at the girder ends. However, a girder is more vulnerable to damage due to a negative bending moment at mid-span than a positive moment at the ends. Therefore, in assessing the girder performance, only the maximum applied negative bending moment in between two supports was considered.

As shown in Table 4, all girders in span 1 failed due to negative moments. In addition to the moment failure, girders 3, 4 and 5 also failed because of inadequate shear capacity. Apparently, girders in span 2 survived from the explosion. The pier cap and both the columns collapsed because of very high resulting moment due to this explosion. Although the girders in span 2 survived, secondary failure was expected due to the failure of the pier cap and the columns. It is evident that the model bridge underwent complete collapse due to Case 1 loading requiring immediate replacement.

7.2. Load case 2

Case 2 blast load, as shown in Fig. 6(a), was defined for an explosion occurring on the middle of the girder span 1.83 m above the deck slab. It was assumed that a 6.10 m by 6.10 m square portion of the slab experienced a vertically downward pressure, considering the 30 degree angle of projection. The three consecutive girders 3, 4 and 5 were affected as a result of this explosion. This pressure was distributed over the girder–slab composite section along the centerline of the girders using 50% and 30% distributions. Girder 4 was subjected to a pressure of 5.1 MPa (Table 1, using 50% distribution), and girders 3 and 5 experienced 3.03 MPa pressure (Table 1, using 30% distribution). The uniformly distributed load was 9.33 MN/m and 5.55 MN/m over girder 4, and girders 3 and 5, respectively, applied on the middle 6.10 m of the span. No direct impact on the pier cap or column due to the explosion on top of the bridge was considered.

The moment diagrams produced by Case 2 load are presented in Fig. 6(a). The maximum positive moment (at girder mid-span) and shear force on girder 4 were 170.45 MN m and 35.43 MN, respectively, while those on girders 3 and 5 were 106.05 MN m and 21.73 MN, respectively. Negative moments at the girder ends were not considered, since the girders are more vulnerable to failure at the mid-span rather than at the ends.

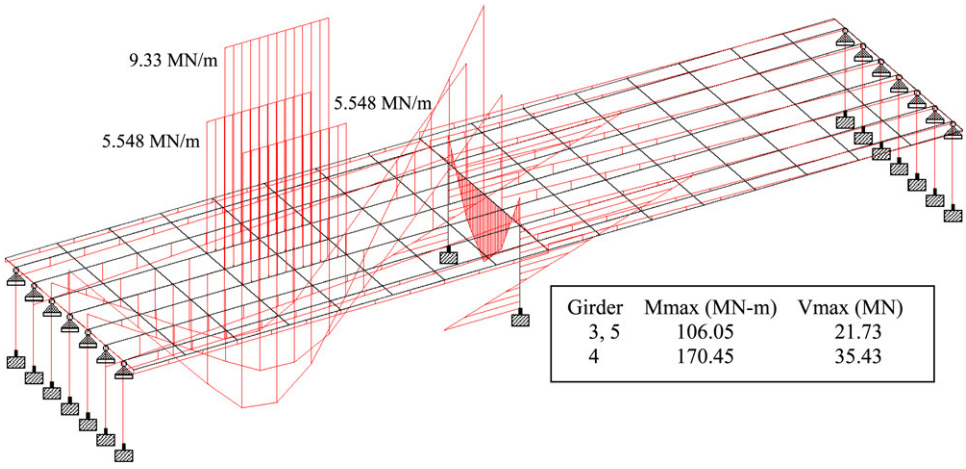

(a) Case II.

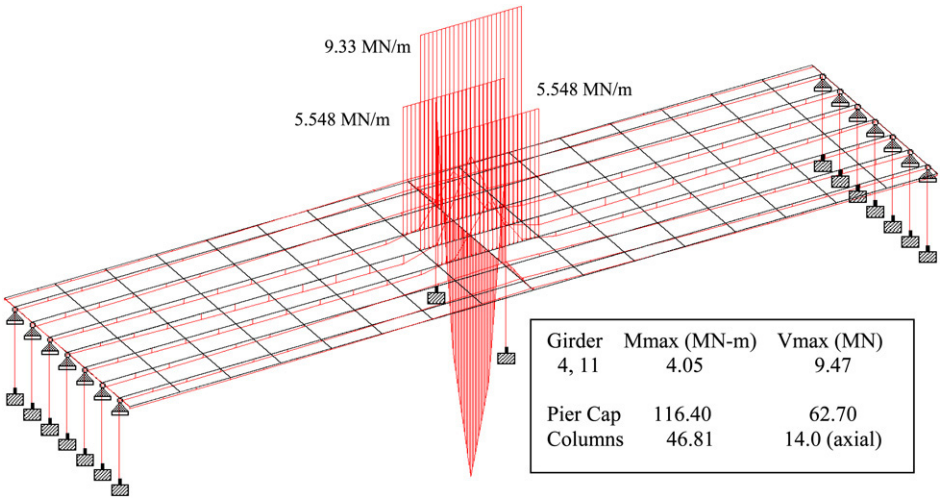

(b) Case III.

Fig. 6. Load and moment diagrams.

Table 4 shows that all girders in span 1 and 2, pier cap and columns collapsed due to Case 2 loading. Very high moments and shears caused failure of all the girders. The columns experienced significant moments and axial forces far beyond their capacity. Girders 2 to 6 experienced shear failure in addition to flexural failure. As a result of Case 2 loading, the model bridge completely collapsed requiring immediate replacement.

7.3. Load case 3

Case 3 blast load, as presented in Fig. 6(b), was identical to Case 2 load, except that the horizontal location was changed to the top of the pier cap. This load was applied on the middle three girders of each span. Girders 4 and 11 were loaded with 9.33 MN/m load for a length of 3.05 m each way from the centerline of the pier cap. In a similar fashion, 5.55 MN/m load was applied on each of the girders 3, 5, 10 and 12.

The maximum positive moment (at pier cap mid-span), as shown in Fig. 6(b) and shear force on the pier cap were 116.40 MN m and 62.70 MN, respectively. The maximum negative moment (on pier cap over column) was 116.39 MN m. The maximum positive moment and shear force in girders 4 and 11 were 4.05 MN m and 9.47 MN, respectively. Columns 1 and 2 experienced identical loads. The maximum negative moment (at column bottom) and axial load were 46.81 MN m and 14.00 MN, respectively.

Girders 3 to 5 and 10 to 12 failed due to the lack of shear capacity under Case 3 loading, as seen from Table 4. None of the girders failed due to the resulting moment. The pier cap and columns failed due to the resulting moment and shears or axial forces. Four girders in each span, which survived from this explosion, were subjected to a secondary failure due to the collapse of the pier cap and the columns. As a result, the whole bridge collapsed requiring immediate replacement.

7.4. Load case 4

Case 4 load, identical to Case 3, was located at the discontinued ends of the girders 3, 4 and 5. This load was applied along the centerline of the girders for a length of 6.10 m from the end bent cap.

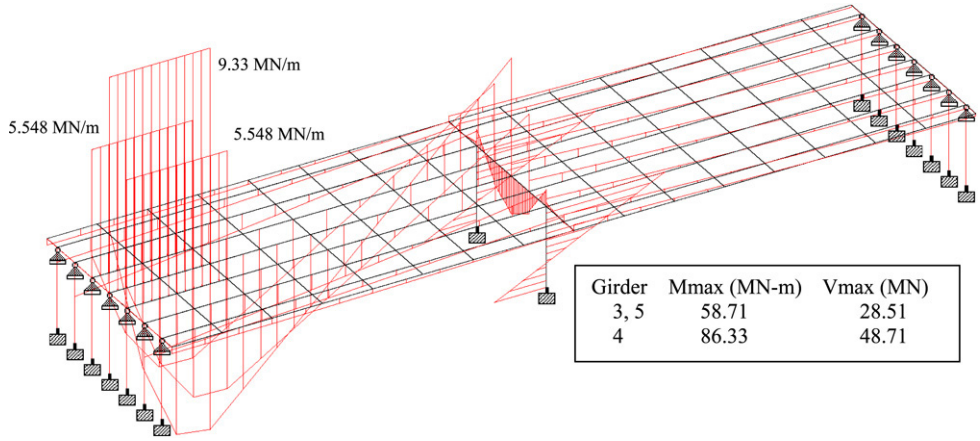

(a) Case IV.

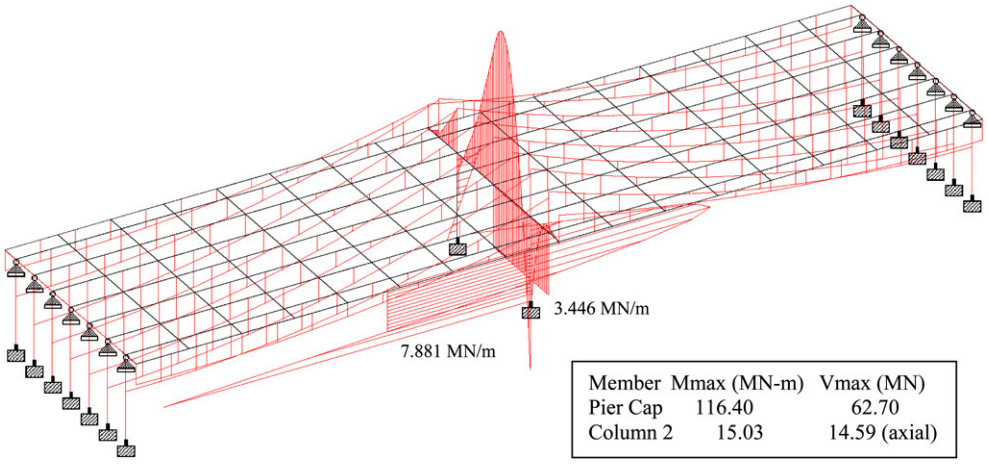

(b) Case V.

Fig. 7. Load and moment diagrams.

Fig. 7(a) presents the bending moment diagrams for Case 4 load. The maximum positive moment and shear force on girder 4 were 86.33 MN m and 48.71 MN, respectively, while those on girders 3 and 5 were 58.71 MN m and 28.51 MN, respectively.

All critical members of the model bridge failed due to the resulting moment generated from Case 4 blast load, as shown in Table 4. Girders in span 1 and span 2 failed due to very high positive and negative moments, respectively. It is noteworthy that the end bent survived the explosion due to the fact that displacement of end bent under vertical blast load was limited due to the supporting actions of soil immediately below the end bent cap. The pier cap and the columns collapsed because of the resulting moment and corresponding shear or axial force. Therefore, the whole bridge collapsed due to Case 4 load necessitating immediate replacement.

7.5. Load case 5

Fig. 7(b) presents Case 5 blast load on the model bridge, which involves horizontal pressure on the column when explosion occurs underneath the bridge at 914 mm above the ground, and at a standoff distance of 1.22 m from the column surface. Since the columns are circular, the total force is less compared to that on a flat surface of equal dimension. Although the projected surface width of the circular column is 1.07 m, as a conservative approach, the equivalent flat surface width of 914 mm was assumed to account for the reduction in the net pressure due to the curved surface. An average intensity of 8.62 MPa (Table 1, using 50% distribution) on the equivalent flat width of 914 mm was applied on the column for a total length of 2.44 m calculated on the basis of 45 degree angle of projection. The converted uniformly distributed load of 7.88 MN/m was applied along the centerline of column 2 for a length of 2.44 m. Simultaneously, the pier cap bottom at 2.74 m above the point of explosion was also subjected to a vertically upward pressure of 2.83 MPa (Table 1, using 50% distribution). In the model, a uniformly distributed load of 3.45 MN/m was applied along the centerline of the pier cap elements 13, 14 and 15. Although the superstructure also captured part of this explosion, it was excluded in this load case analysis.

Fig. 7(b) presents the bending moment diagrams generated by Case 5 load. The maximum negative bending moment and axial force produced by these loads on column 2 were 15.03 MN m and 14.59 MN, respectively. The maximum negative bending moment and shear force on the pier cap elements

were 6.54 MN m (element 13) and 9.15 MN (element 14), respectively.

As noted in Table 4, girders 2 to 6 and 9 to 14 failed due to negative moments, which may result in minor cracks on top of the bridge slab. The rest of the girders survived the explosion. The pier cap and column 2 failed, while column 1 survived. No shear failure was observed. Because of one column failure and minor cracks on top of the bridge, the whole bridge may not immediately collapse. Depending on the magnitude, location and amount of damage, the bridge was identified as completely out of service and required emergency repair works.

8. Limitations of analysis

Although blast load is a dynamic load and it impacts the structure for a very short duration, equivalent static loads due to explosion were used herein in assessing the structural performance. There may be some minor variation in the results between equivalent static and dynamic analysis of the model bridge because of impact and sustained loading, but the overall performance of a structure would be fairly close in each of these two types of analyses. If a structure fails due to a static load, it is likely to fail due to the equivalent amount of dynamic load for any duration. Although earthquakes produce dynamic loads, similar analogy of converting dynamic loads into static loads has been used with acceptable accuracy for structural design. Therefore, performance of bridge elements under equivalent static loads may be considered as conservatively similar to that under the original dynamic blast load.

Typical smaller AASHTO girders are normally simply supported. They are, however, compositely connected through the cast-in-place slab. This makes the girders partly continuous over the pier support, generating end moments. Moments at the pier supports were produced because of the structural continuity formed by the deck slab. Small moments were observed at the girder ends in the model output. This is most likely due to the combined action of the superstructure stiffness produced by the strong framing action between the deck slab and the girders, and the high dead loads of the superstructure sustained by the simple end supports.

Because of the application limitations in the STAAD.Pro software, only the centerline of each bridge element was modeled herein. The equivalent area of the girders and barriers were used in the analysis in finding resulting moment and shear forces. Generally, the shape of the structure does not interfere with calculating the applied loads on the structure. The self-weight of the elements depends only on the cross-sectional area magnitudes. All static blast loads were converted to equivalent uniformly distributed loads and applied at the centerline of each bridge element, which also did not affect the analysis accuracy.

9. Experimental validation

An effort was made to validate the theoretical modeling performed in this research with available experimental results. An extensive literature review was performed herein for this purpose. The search could not locate any full-scale blast load test on bridge structures except for demolition purposes only. Some real life blast tests were conducted on experimental buildings; however, as these data are very sensitive and confidential for security reasons, they are not available to the public. Several attempts were made to legally collect some blast test data in order to validate the ATBlast and STAAD.Pro models developed herein, but no viable response was received from these sources.

10. Conclusion

Based on this research, the following conclusions may be made:

1. To protect bridges from the act of terrorist explosion, blast resistant bridge design and retrofit techniques should be developed and adopted by the applicable code and regulatory agencies.
2. It was found from the analytical study that a typical Type III AASHTO girder bridge will fail due to a probable blast load generated by an explosion of 226.8 kg of TNT and applied underneath or over the bridge at girder end or mid-span. In general, AASHTO girder bridges are vulnerable to failure under blast loading.
3. Part of the bridge is expected to survive the explosion when the blast load is applied at a location close to the column, which includes blast loads applied directly on one column and a portion of the pier cap.
4. With a blast occurrence under one span or over the pier cap, some of the girders on the other span are expected to survive the explosion.
5. In case the typical blast is set off on the pier or column, the components underwent immediate failure.
6. It was determined from the research that the Type III AASHTO girders, traditionally designed pier cap and column could not withstand the impact of 226.8 kg of TNT. In summary, AASHTO girder bridges with concrete columns and piers are not capable of resisting specific blast load.

Appendix A. Distribution of blast loading — case I

See Fig. A.1.

$$\begin{aligned}\mathrm{Load}_{\mathrm{Beam29}} &:= [P_0 \cdot 4 + P_1 \cdot 12 + P_2 \cdot 20 \\ &\quad + (P_3 + P_4 + P_5 + P_6 + P_7 + P_8) \cdot 12] \\ &\quad \cdot 144 \cdot \frac{\mathrm{kip}}{20 \cdot \mathrm{ft}}\end{aligned}$$

$$\mathrm{Load}_{\mathrm{Beam29}} = 664 \frac{\mathrm{kip}}{\mathrm{ft}}$$

$$\begin{aligned}\mathrm{Load}_{\mathrm{Beam30}} &:= (P_3 \cdot 8 + P_4 \cdot 12 + P_5 \cdot 16 + P_6 \cdot 20 + P_7 \cdot 24 \\ &\quad + P_8 \cdot 28 + P_9 \cdot 12) \cdot 144 \cdot \frac{\mathrm{kip}}{20 \cdot \mathrm{ft}}\end{aligned}$$

$$\mathrm{Load}_{\mathrm{Beam30}} = 441 \frac{\mathrm{kip}}{\mathrm{ft}}$$

$$\mathrm{Pressure}_{\mathrm{Beam29}} := \frac{\mathrm{Pressure}_{\mathrm{Beam29}}}{6 \cdot \mathrm{ft}}$$

$$\mathrm{Pressure}_{\mathrm{Beam29}} := 0.77\ \mathrm{ksi}$$

Explosive Amount = 500 lb (226.8 kg) TNT

$Y := 6 \qquad i := 0, 1 .. 9$

$X_i := i + 1 \qquad d_i := \sqrt{Y^2 + (X_i)^2}$

$\theta_i := \operatorname{asin}\left(\frac{Y}{d_i}\right) \qquad kip \equiv 1000 \cdot lb \qquad ksi := \frac{kip}{in^2}$

$d =$

	0
0	6.083
1	6.325
2	6.708
3	7.211
4	7.81
5	8.485
6	9.22
7	10
8	10.817
9	11.662

$\theta =$

	0
0	80.538
1	71.565
2	63.435
3	56.31
4	50.194
5	45
6	40.601
7	36.87
8	33.69
9	30.964

deg

$F :=$

3.576
2.511
1.884
1.480
1.198
0.991
0.832
0.707
0.606
0.524
0.456
0.398
0.350
0.309
0.275
0.245
0.219
0.196
0.177
0.161
0.145
0.132
0.121

$P_0 := \left[F_3 - (F_3 - F_4)\cdot(d_0 - 6)\right]\cdot\sin(\theta_0) \qquad P_0 = 1.437$

$P_1 := \left[F_3 - (F_3 - F_4)\cdot(d_1 - 6)\right]\cdot\sin(\theta_1) \qquad P_1 = 1.317$

$P_2 := \left[F_3 - (F_3 - F_4)\cdot(d_2 - 6)\right]\cdot\sin(\theta_2) \qquad P_2 = 1.145$

$P_3 := \left[F_4 - (F_4 - F_5)\cdot(d_3 - 7)\right]\cdot\sin(\theta_3) \qquad P_3 = 0.96$

$P_4 := \left[F_4 - (F_4 - F_5)\cdot(d_4 - 7)\right]\cdot\sin(\theta_4) \qquad P_4 = 0.791$

$P_5 := \left[F_5 - (F_5 - F_6)\cdot(d_5 - 8)\right]\cdot\sin(\theta_5) \qquad P_5 = 0.646$

$P_6 := \left[F_6 - (F_6 - F_7)\cdot(d_6 - 9)\right]\cdot\sin(\theta_6) \qquad P_6 = 0.524$

$P_7 := F_7\cdot\sin(\theta_7) \qquad P_7 = 0.424$

$P_8 := \left[F_7 - (F_7 - F_8)\cdot(d_8 - 10)\right]\cdot\sin(\theta_8) \qquad P_8 = 0.346$

$P_9 := \left[F_8 - (F_8 - F_9)\cdot(d_9 - 11)\right]\cdot\sin(\theta_9) \qquad P_9 = 0.284$

Fig. A.1.

which is approximately 50% of maximum pressure of 1.48 ksi.

$\text{Pressure}_{\text{Beam30}} := \frac{\text{Load}_{\text{Beam30}}}{6 \cdot ft}$

$\text{Pressure}_{\text{Beam30}} = 0.51\ ksi$

which is approximately 30% of the maximum pressure of 1.48 ksi.

Appendix B. Distribution of blast loading — case II

See Fig. B.1.

$$\text{Load}_{\text{Beam29}} := [P_0 \cdot 4 + P_1 \cdot 12 + P_2 \cdot 20 + (P_3 + P_4 + P_5 + P_6 + P_7 + P_8) \cdot 12] \cdot 144 \cdot \frac{kip}{20 \cdot ft}$$

Explosive Amount = 100 lb (45.4 kg) TNT

$Y := 6 \qquad i := 0, 1 .. 9 \qquad k := 0, 1 .. 22$

$X_i := i + 1 \qquad d_i := \sqrt{Y^2 + (X_i)^2} \qquad R_k := k + 3$

$\theta_i := \operatorname{asin}\left(\frac{Y}{d_i}\right) \qquad kip \equiv 1000 \cdot lb \qquad ksi := \frac{kip}{in^2}$

$d =$

	0
0	6.083
1	6.325
2	6.708
3	7.211
4	7.81
5	8.485
6	9.22
7	10
8	10.817
9	11.662

$\theta =$

	0
0	80.538
1	71.565
2	63.435
3	56.31
4	50.194
5	45
6	40.601
7	36.87
8	33.69
9	30.964

deg

$R =$

	0	1
0	3	
1	4	
2	5	
3	6	
4	7	
5	8	
6	9	
7	10	
8	11	
9	12	
10	13	
11	14	
12	15	
13	16	
14	17	
15	18	
16	19	
17	20	
18	21	
19	22	
20	23	
21	24	
22	25	

$F :=$

1.821
1.237
0.898
0.679
0.526
0.416
0.334
0.271
0.223
0.186
0.156
0.133
0.114
0.098
0.085
0.075
0.066
0.059
0.052
0.047
0.042
0.038
0.035

$P_0 := \left[F_3 - (F_3 - F_4)\cdot(d_0 - 6)\right]\cdot\sin(\theta_0) \qquad P_0 = 0.657$

$P_1 := \left[F_3 - (F_3 - F_4)\cdot(d_1 - 6)\right]\cdot\sin(\theta_1) \qquad P_1 = 0.597$

$P_2 := \left[F_3 - (F_3 - F_4)\cdot(d_2 - 6)\right]\cdot\sin(\theta_2) \qquad P_2 = 0.51$

$P_3 := \left[F_4 - (F_4 - F_5)\cdot(d_3 - 7)\right]\cdot\sin(\theta_3) \qquad P_3 = 0.418$

$P_4 := \left[F_4 - (F_4 - F_5)\cdot(d_4 - 7)\right]\cdot\sin(\theta_4) \qquad P_4 = 0.336$

$P_5 := \left[F_5 - (F_5 - F_6)\cdot(d_5 - 8)\right]\cdot\sin(\theta_5) \qquad P_5 = 0.266$

$P_6 := \left[F_6 - (F_6 - F_7)\cdot(d_6 - 9)\right]\cdot\sin(\theta_6) \qquad P_6 = 0.208$

$P_7 := F_7\cdot\sin(\theta_7) \qquad P_7 = 0.163$

$P_8 := \left[F_7 - (F_7 - F_8)\cdot(d_8 - 10)\right]\cdot\sin(\theta_8) \qquad P_8 = 0.129$

$P_9 := \left[F_8 - (F_8 - F_9)\cdot(d_9 - 11)\right]\cdot\sin(\theta_9) \qquad P_9 = 0.102$

Fig. B.1.

$Load_{Beam29} = 284\frac{kip}{ft}$

$Load_{Beam30} := (P_3 \cdot 8 + P_4 \cdot 12 + P_5 \cdot 16 + P_6 \cdot 20 + P_7 \cdot 24 + P_8 \cdot 28 + P_9 \cdot 12) \cdot 144 \cdot \frac{kip}{20 \cdot ft}$

$Load_{Beam30} = 177\frac{kip}{ft}$

$Pressure_{Beam29} := \frac{Pressure_{Beam29}}{6 \cdot ft}$

$Pressure_{Beam29} := 0.329\ ksi$

Explosive Amount = 50 lb (22.7 kg) TNT

$Y := 6 \qquad i := 0, 1 .. 9 \qquad k := 0, 1 .. 22$

$X_i := i + 1 \qquad d_i := \sqrt{Y^2 + (X_i)^2} \qquad R_k := k + 3$

$\theta_i := \operatorname{asin}\left(\frac{Y}{d_i}\right) \qquad kip \equiv 1000\,lb \qquad ksi := \frac{kip}{in^2}$

$d =$

	0
0	6.083
1	6.325
2	6.708
3	7.211
4	7.81
5	8.485
6	9.22
7	10
8	10.817
9	11.662

$\theta =$

	0
0	80.538
1	71.565
2	63.435
3	56.31
4	50.194
5	45
6	40.601
7	36.87
8	33.69
9	30.964

deg

$R =$

	0	1
0	3	
1	4	
2	5	
3	6	
4	7	
5	8	
6	9	
7	10	
8	11	
9	12	
10	13	
11	14	
12	15	
13	16	
14	17	
15	18	
16	19	
17	20	
18	21	
19	22	
20	23	
21	24	
22	25	

$F := \begin{pmatrix} 1.337 \\ 0.888 \\ 0.627 \\ 0.460 \\ 0.347 \\ 0.267 \\ 0.210 \\ 0.167 \\ 0.136 \\ 0.112 \\ 0.093 \\ 0.078 \\ 0.067 \\ 0.058 \\ 0.050 \\ 0.044 \\ 0.039 \\ 0.034 \\ 0.031 \\ 0.028 \\ 0.025 \\ 0.023 \\ 0.021 \end{pmatrix}$

$P_0 := \left[F_3 - (F_3 - F_4)\cdot(d_0 - 6)\right]\cdot\sin(\theta_0) \qquad P_0 = 0.445$

$P_1 := \left[F_3 - (F_3 - F_4)\cdot(d_1 - 6)\right]\cdot\sin(\theta_1) \qquad P_1 = 0.402$

$P_2 := \left[F_3 - (F_3 - F_4)\cdot(d_2 - 6)\right]\cdot\sin(\theta_2) \qquad P_2 = 0.34$

$P_3 := \left[F_4 - (F_4 - F_5)\cdot(d_3 - 7)\right]\cdot\sin(\theta_3) \qquad P_3 = 0.275$

$P_4 := \left[F_4 - (F_4 - F_5)\cdot(d_4 - 7)\right]\cdot\sin(\theta_4) \qquad P_4 = 0.217$

$P_5 := \left[F_5 - (F_5 - F_6)\cdot(d_5 - 8)\right]\cdot\sin(\theta_5) \qquad P_5 = 0.169$

$P_6 := \left[F_6 - (F_6 - F_7)\cdot(d_6 - 9)\right]\cdot\sin(\theta_6) \qquad P_6 = 0.131$

$P_7 := F_7\cdot\sin(\theta_7) \qquad P_7 = 0.1$

$P_8 := \left[F_7 - (F_7 - F_8)\cdot(d_8 - 10)\right]\cdot\sin(\theta_8) \qquad P_8 = 0.079$

$P_9 := \left[F_8 - (F_8 - F_9)\cdot(d_9 - 11)\right]\cdot\sin(\theta_9) \qquad P_9 = 0.062$

Fig. C.1.

which is approximately 50% of maximum pressure of 0.679 ksi.

$\text{Pressure}_{\text{Beam30}} := \frac{\text{Load}_{\text{Beam30}}}{6\cdot ft}$

$\text{Pressure}_{\text{Beam30}} = 0.204\ ksi$

which is approximately 30% of maximum pressure of 0.697 ksi.

Appendix C. Distribution of blast loading — case III

See Fig. C.1.

$\text{Load}_{\text{Beam29}} := [P_0\cdot 4 + P_1\cdot 12 + P_2\cdot 20 + (P_3 + P_4 + P_5 + P_6 + P_7 + P_8)\cdot 12]\cdot 144\cdot\frac{kip}{20\cdot ft}$

$$\text{Load}_{\text{Beam29}} = 186\frac{\text{kip}}{\text{ft}}$$

$$\text{Load}_{\text{Beam30}} := (P_3 \cdot 8 + P_4 \cdot 12 + P_5 \cdot 16 + P_6 \cdot 20 + P_7 \cdot 24 + P_8 \cdot 28 + P_9 \cdot 12) \cdot 144 \cdot \frac{\text{kip}}{20 \cdot \text{ft}}$$

$$\text{Load}_{\text{Beam30}} = 111\frac{\text{kip}}{\text{ft}}$$

$$\text{Pressure}_{\text{Beam29}} := \frac{\text{Pressure}_{\text{Beam29}}}{6 \cdot \text{ft}}$$

$$\text{Pressure}_{\text{Beam29}} := 215\ \text{ksi}$$

which is approximately 50% of maximum pressure of 0.460 ksi.

$$\text{Pressure}_{\text{Beam30}} := \frac{\text{Load}_{\text{Beam30}}}{6 \cdot \text{ft}}$$

$$\text{Pressure}_{\text{Beam30}} = 0.129\ \text{ksi}$$

which is approximately 30% of maximum pressure of 0.460 ksi.

References

[1] Recommendation for bridge and tunnel security, AASHTO Blue Ribbon Panel on Bridge and Tunnel Security. 2003.

[2] National cooperative highway research program, Project no. 12–72. 2005.

[3] Design of blast resistant buildings in petrochemical facilities, ASCE Task Committee on Blast Resistant Design. 1997.

[4] Explosion effects and structural design for blast, A Two-Day Training Course, National Center for Explosion Resistant Design, Department of Civil and Environmental Engineering, University of Missouri-Columbia. 2005.

[5] Marchand K, Williamson EB, Winget DG. Analysis of blast load on bridge substructures. Structures under shock and impact VIII. Wessex Institute of Technology Press, WIT Press; 2004.

[6] Load and Resistant Factor Design. Bridge Design Specifications, American Association of State Highway and Officials; 2003.

[7] Florida department of transportation, LRFD Prestressed Beam Program, English v1.85. 2001.

[8] LEAP software, Inc., RC-Pier 2001. Tampa, Florida.

[9] Florida department of transportation, Biaxial Column Program, v2.3. 2001.

[10] TM 5-1300, Structures to Resist the Effects of Accidental Explosions, US Department of Defense. 1990.

[11] ATBlast software, Developed by Applied Research Associates (ARA), Inc. 2003.

[12] Research engineers international, STAAD.Pro 2004, USA. 2004.